

## Search for $H^\pm \rightarrow \tau_{\text{had}}^\pm + \nu$ in ATLAS

---

**Patrick CZODROWSKI\***

On behalf of the ATLAS Collaboration

*Technische Universität Dresden*

*E-mail:* Patrick.Czodrowski@tu-dresden.de

Decays of top quarks in  $4.6 \text{ fb}^{-1}$  of proton-proton collisions data at  $\sqrt{s} = 7 \text{ TeV}$  collected by the ATLAS experiment at the Large Hadron Collider at CERN were selected and analyzed to search for signatures of charged Higgs bosons with a hadronically decaying  $\tau$  lepton in the final state. The data are consistent with the expected background from Standard Model processes. Assuming a branching ratio of the charged Higgs boson to a  $\tau$  lepton and a neutrino of 100% and combining with the leptonically decaying  $\tau$  analysis, upper limits on the branching ratio of top quark decays to a  $b$  quark and a charged Higgs boson between 5% and 1% are obtained for charged Higgs boson masses ranging from 90 GeV to 160 GeV, respectively. In the context of the  $m_h^{\text{max}}$  scenario of the MSSM,  $\tan\beta$  above 12–26, as well as between 1 and 2–6, can be excluded for charged Higgs boson masses between 90 GeV and 150 GeV.

*Prospects for Charged Higgs Discovery at Colliders*

*October 8-11, 2012*

*Uppsala University Sweden*

---

\*Speaker.

## 1. Introduction

The charged Higgs boson is predicted by many scenarios with an extended Higgs sector, such as models containing Higgs triplets, Two-Higgs-Doublet Models (2HDM) [1] and supersymmetric models. An observation of charged Higgs bosons,  $H^\pm$ , would indicate physics beyond the Standard Model (SM). Both analyses presented here consider the type-II 2HDM, which is also the Higgs sector of the Minimal Supersymmetric Standard Model (MSSM). For charged Higgs boson masses,  $m_{H^\pm}$ , smaller than the top quark mass,  $m_t$ , the dominant production mode at the Large Hadron Collider (LHC) for  $H^\pm$  is through top quark decay via  $t \rightarrow bH^+$ . The dominant source of top quarks at the LHC is  $t\bar{t}$  production, as shown by the example Feynman diagram in Figure 1.

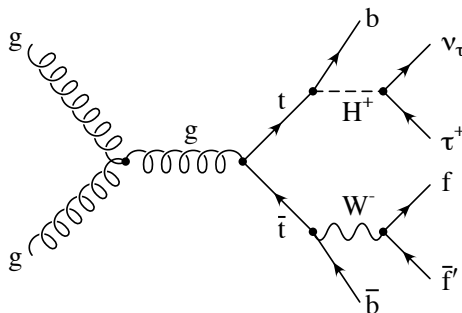


**Figure 1:** Example for a leading-order Feynman diagram for the production of a charged Higgs boson through gluon fusion in  $t\bar{t}$  decays. [3]

Tau leptons ( $\tau$  leptons) play a crucial role in many physics processes investigated by the ATLAS (A Toroidal LHC ApparatuS) experiment [2] at the LHC, within the SM and beyond. They have a branching ratio into hadronic decay modes of approximately 65% and 35% into leptonic modes (electron or muon accompanied by two neutrinos). As the leptonically decaying  $\tau$  leptons cannot be distinguished from prompt leptons, only hadronically decaying  $\tau$  leptons are considered from now on. Hadronically decaying  $\tau$  leptons here are denoted by the term  $\tau$  leptons, unless stated otherwise this implies  $\tau^+$  and  $\tau^-$ . The main hadronic decay channels contain one or three charged hadrons, most of them pions and a small amount of kaons, with additional neutral pions or kaons, as well as a neutrino. This article is based upon the ATLAS publication [3]. A charged Higgs analysis studying the leptonically decaying  $\tau$  leptons exists, also documented in Reference [3].

## 2. Background Estimations

This section introduces data-driven background estimation methods utilized in the presented analyses. For further details please refer to Reference [3].

### 2.1 The Embedding Method

The method consists in selecting a control sample of  $t\bar{t}$ , single-top and  $W$ +jets events with a reconstructed muon and replacing the detector signature of this muon with that of a simulated  $\tau$  lepton. Reconstruction algorithms are then re-applied to the new hybrid events, which are thereafter used to estimate the background arising from SM processes with correctly reconstructed  $\tau$  leptons.

The whole event (except for the  $\tau$  leptons) is thus taken directly from data, including underlying event and pile-up, missing energy,  $b$  quark and light quark jets. In Figure 2 the prediction of the embedding method, compared to Monte Carlo simulation, for the transverse mass<sup>1</sup>,  $m_T$ , variable for correctly reconstructed  $\tau$  leptons is shown.

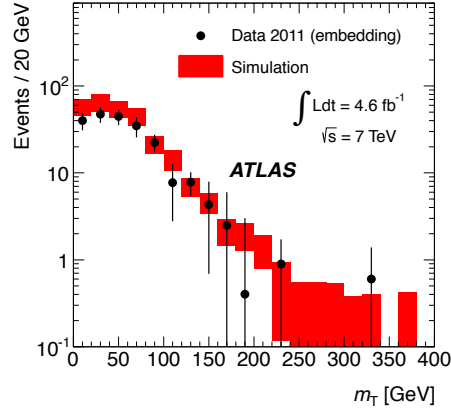


**Figure 2:** Comparison of the  $m_T$  distribution for correctly reconstructed  $\tau$  leptons, predicted by the embedding method and by simulation. Combined statistical and systematic uncertainties are shown. [3]

## 2.2 Backgrounds with jets and electrons misidentified as $\tau$ leptons

The probability measured in data for a jet to be misidentified as a hadronically decaying  $\tau$  lepton is used to predict the yield of events with misidentified  $\tau$  leptons from the most important SM backgrounds. A control sample enriched with  $W$ +jets events is selected to measure the jet-to- $\tau$  probability. An example of the prediction of this method is given and compared to the Monte Carlo simulation in Table 1. The background of electrons misidentified as  $\tau$  leptons is estimated selecting a  $Z \rightarrow e^+e^-$  control region in the data [4], where either the electron or the positron is reconstructed as a hadronically decaying  $\tau$  lepton. The measured misidentification probabilities, which have an average value of 0.2%, are then applied to all simulated events in the  $\tau$ +lepton analysis, described in detail in Section 4. Simulation studies show that this application is valid, as the electron-to- $\tau$  misidentification probabilities for  $Z \rightarrow e^+e^-$  and  $t\bar{t}$  events agree well.

| Sample           | Data-driven method [events] | Simulation [events] |
|------------------|-----------------------------|---------------------|
| $t\bar{t}$       | $33 \pm 1$                  | $37 \pm 1$          |
| $W$ +jets        | $2.5 \pm 0.1$               | $3.9 \pm 1.5$       |
| Single top quark | $1.3 \pm 0.1$               | $2.0 \pm 0.3$       |

**Table 1:** Estimated number of background events in the  $\tau$ +jets analysis in  $4.6 \text{ fb}^{-1}$  of data using the data-driven method and Monte Carlo simulation. [3]

<sup>1</sup> $m_T = \sqrt{2p_T^\tau E_T^{\text{miss}}(1 - \cos \Delta\phi_{\tau, \text{miss}})}$ , where  $\Delta\phi_{\tau, \text{miss}}$  is the azimuthal angle between the  $\tau$  and the direction of the missing transverse momentum.

## 2.3 Multi-Jet Background Estimation

The multi-jet background is estimated by adjusting its rate such that the  $E_T^{\text{miss}}$  distribution of the sum of the data-derived QCD-template and other simulated processes agree well with the data. A control region is defined where the  $\tau$  leptons must pass a looser  $\tau$  identification, but fail the tighter  $\tau$  identification [5] of the default selection. Furthermore the events are required not to contain any  $b$ -tagged jet. Under the assumption that the shapes of the  $E_T^{\text{miss}}$  and  $m_T$  distributions are the same in control and signal regions, the  $E_T^{\text{miss}}$  shape of the multi-jet background is measured in the control region, after subtracting the simulated background contributions from other processes. These amount to less than 1% of the observed events in the control region. Figure 3(a) compares the  $E_T^{\text{miss}}$  shapes obtained with the  $\tau$ +jets selection and in the control region just before the final  $E_T^{\text{miss}}$  requirement of the selection. The differences between the two distributions are taken into account as systematic uncertainty of this estimation method. A simultaneous fit is then performed on the  $E_T^{\text{miss}}$  distribution of the selected data. The first fit-template is the multi-jet model obtained from the control region and the second template is the shape of the sum of the other processes (in this case dominated by  $t\bar{t}$  and  $W$ +jets) from Monte Carlo simulation. The fit result is shown in Figure 3(b).

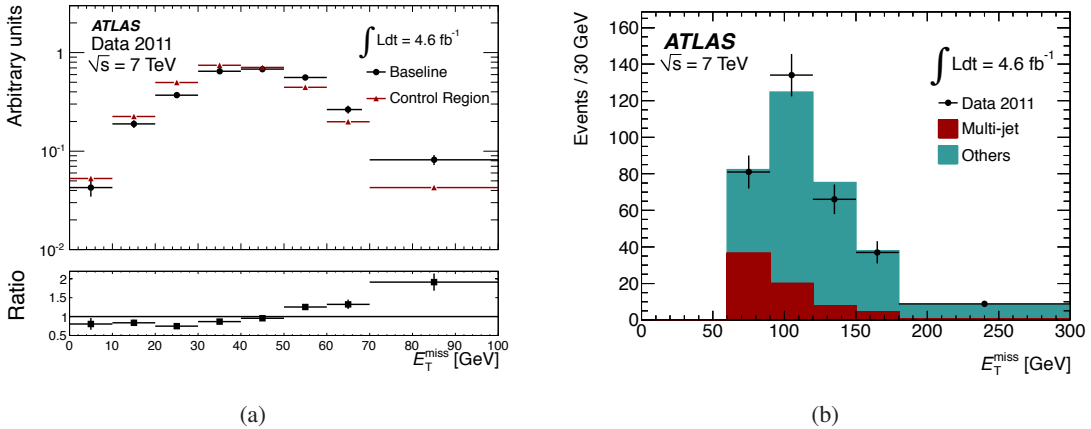


**Figure 3:** (a) Shape of  $E_T^{\text{miss}}$  in the data control region after the baseline selection (before the  $E_T^{\text{miss}}$  requirement) and after subtracting the simulated expectation from  $t\bar{t}$ ,  $W$ +jets, and single top quark processes. (b) Fit of the  $E_T^{\text{miss}}$  templates in the signal region to data. Here only statistical uncertainties are given. [3]

## 3. $\tau$ +jets Analysis

### 3.1 Analysis Strategy

This analysis relies on the detection of  $\tau$ +jets decays of  $t\bar{t}$  events. The hadronically decaying  $\tau$  lepton arises from the  $H^\pm \rightarrow \tau_{\text{had}}^\pm \nu$  decay, while the jets stem from a hadronically decaying  $W$  boson, i.e.  $t\bar{t} \rightarrow b\bar{b}WH^+ \rightarrow b\bar{b}(q\bar{q}')(\tau_{\text{had}}\nu)$ . For the selected events, the transverse mass,  $m_T$ , is used as final discriminating variable. It is related to the  $W^\pm$  boson mass, therefore the discriminating power grows with the increasing mass difference of the  $H^\pm$  signal and the  $W^\pm$  bosons in  $t\bar{t}$  background decays.

### 3.2 Event selection

The  $\tau$ +jets analysis uses events passing a  $\tau + E_T^{\text{miss}}$  trigger described in [6] with a threshold of 29 GeV on the  $\tau$  trigger object and 35 GeV on the calorimeter-based  $E_T^{\text{miss}}$ . The following requirements are applied, in that respective order:

- at least four jets (excluding  $\tau$  leptons) with  $p_T > 20$  GeV, among these at least one  $b$ -tagged jet;
- exactly one  $\tau$  with  $p_T > 40$  GeV, within  $|\eta| < 2.3$  and matching the corresponding  $\tau$  trigger object;
- neither a second  $\tau$  with  $p_T > 20$  GeV, nor any electrons with  $E_T > 20$  GeV, nor any muons with  $p_T > 15$  GeV;
- $E_T^{\text{miss}} > 65$  GeV;
- to reject events in which a large reconstructed  $E_T^{\text{miss}}$  is due to the limited resolution of the energy measurement, the following ratio, based on the  $\sum p_T$  must satisfy<sup>2</sup>:

$$\frac{E_T^{\text{miss}}}{0.5 \text{ GeV}^{1/2} \cdot \sqrt{\sum p_T}} > 13;$$

- a topology consistent with a top quark decay; this is ensured by the combination of one  $b$ -tagged jet ( $b$ ) and two untagged jets ( $j$ ) with the highest  $p_T^{j\bar{j}b}$  satisfying  $m_{j\bar{j}b} \in [120, 240]$  GeV.

### 3.3 Event Yield

Table 2 gives the expected number of background events for the SM-only hypothesis and the observation in the data. The total number of predicted events (signal+background) in the presence of a 130 GeV charged Higgs boson with  $\mathcal{B}(t \rightarrow bH^+) = 5\%$  is given in the last rows. The number of events with a correctly reconstructed  $\tau$  lepton, labeled "true  $\tau$ ", is derived from the number of embedded events. In the presence of a charged Higgs boson in the top quark decays the contributions of  $t\bar{t} \rightarrow b\bar{b}W^+W^-$  events in these backgrounds are scaled according to  $\mathcal{B}(t \rightarrow bH^+)$ . The data are found to be consistent with the the SM background estimation. The  $m_T$  distribution for the  $\tau$ +jets channel, after all selection cuts, is shown in Figure 4.

## 4. $\tau$ +lepton Analysis

### 4.1 Analysis Strategy

This analysis relies on the detection of  $\tau$ +lepton decays of  $t\bar{t}$  events, where the hadronically decaying  $\tau$  lepton arises from  $H^\pm \rightarrow \tau_{\text{had}}^\pm \nu$ , while the electron or muon stem from the decay of the  $W$  boson, i.e.  $t\bar{t} \rightarrow b\bar{b}WH^+ \rightarrow b\bar{b}(l\nu)(\tau_{\text{had}}\nu)$ . In this analysis  $E_T^{\text{miss}}$  is used as the discriminating variable between SM  $t\bar{t}$  events and those where the top quark decays are mediated via a charged Higgs boson, in which case the neutrinos are likely to carry away more energy.

<sup>2</sup> $\sum p_T$  is the sum of the transverse momenta of all tracks associated with the primary vertex. Tracks entering the sum must pass quality cuts on the number of hits in the central tracking detector and have  $p_T > 1$  GeV. As this variable is based on tracks from the primary vertex (as opposed to energy deposits in the calorimeter), it is robust against pile-up.

| Sample                               | Event yield ( $\tau$ +jets) |
|--------------------------------------|-----------------------------|
| True $\tau$ (embedding method)       | $210 \pm 10 \pm 44$         |
| Misidentified jet $\rightarrow \tau$ | $36 \pm 6 \pm 10$           |
| Misidentified $e \rightarrow \tau$   | $3 \pm 1 \pm 1$             |
| Multi-jet processes                  | $74 \pm 3 \pm 47$           |
| All SM backgrounds                   | $330 \pm 12 \pm 65$         |
| Data                                 | 355                         |
| $t \rightarrow bH^+$ (130 GeV)       | $220 \pm 6 \pm 56$          |
| Signal+background                    | $540 \pm 13 \pm 85$         |

**Table 2:** Expected event yields after all selection cuts in the  $\tau$ +jets channel and comparison with  $4.6 \text{ fb}^{-1}$  of data. The numbers in the last two rows, for a hypothetical  $H^+$  signal with  $m_{H^\pm} = 130 \text{ GeV}$ , are obtained by assuming  $\mathcal{B}(t \rightarrow bH^+) = 5\%$ . The rows for the backgrounds with misidentified objects assume  $\mathcal{B}(t \rightarrow bW) = 100\%$ . Both statistical and systematic uncertainties are shown, in that respective order. [3]

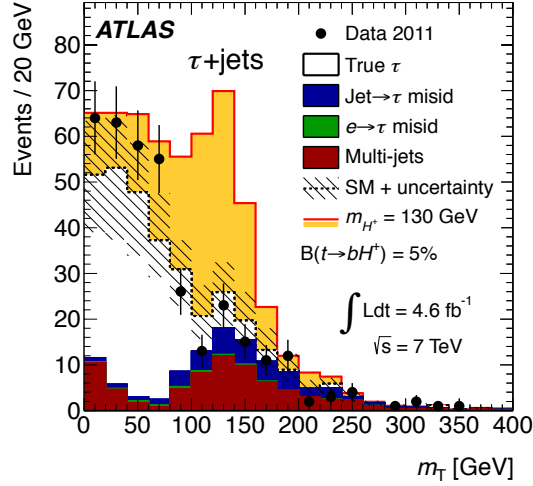


**Figure 4:** Distribution of  $m_T$  after all selection cuts in the  $\tau$ +jets channel. The dashed line corresponds to the SM-only hypothesis and the hatched area around it shows the total uncertainty for the SM backgrounds. The solid line shows the predicted contribution of signal+background in the presence of a charged Higgs boson with  $m_{H^\pm} = 130 \text{ GeV}$ , assuming  $\mathcal{B}(t \rightarrow bH^+) = 5\%$  and  $\mathcal{B}(H^\pm \rightarrow \tau^\pm \nu) = 100\%$ . The contributions of  $t\bar{t} \rightarrow b\bar{b}W^+W^-$  events in the backgrounds with misidentified objects are scaled down accordingly. [3]

## 4.2 Event Selection

The  $\tau$ +lepton analysis uses single-lepton triggers described in [6]. In order to select  $\tau$ +lepton events, the following requirements are imposed:

- exactly one lepton, with  $E_T > 25 \text{ GeV}$  (electron) or  $p_T > 20 \text{ GeV}$  (muon) and matched to the corresponding trigger object, no further electron or muon present in the event;
- exactly one  $\tau$  with  $p_T > 20 \text{ GeV}$  and an electric charge opposite to the selected lepton;

- at least two jets with  $p_T > 20$  GeV, of these at least one  $b$ -tagged jet;
- $\sum p_T > 100$  GeV; in order to suppress multi-jet events.

### 4.3 Event Yields

Table 3 gives the expected number of background events for the SM-only hypothesis and the observation in the data. The total number of predicted events (signal+background) in the presence of a 130 GeV charged Higgs boson with  $\mathcal{B}(t \rightarrow bH^+) = 5\%$  is also stated. In the presence of a charged Higgs boson in the top quark decays, with a branching ratio  $\mathcal{B}(t \rightarrow bH^+)$ , the contributions of  $t\bar{t} \rightarrow b\bar{b}W^+W^-$  events in the backgrounds with true or misidentified  $\tau$  leptons are scaled accordingly. The background with correctly reconstructed  $\tau$  leptons, in this channel, is obtained from simulation, denoted by "true  $\tau$ +lepton" in Table 3. The data are found to be consistent with the expectation for the background-only hypothesis. The  $E_T^{\text{miss}}$  distributions for the  $\tau + e$  and  $\tau + \mu$  channels after all selection cuts applied are shown in Figure 5.

| Sample                               | Event yield ( $\tau$ +lepton) |                       |
|--------------------------------------|-------------------------------|-----------------------|
|                                      | $\tau + e$                    | $\tau + \mu$          |
| True $\tau$ +lepton                  | $430 \pm 14 \pm 59$           | $570 \pm 15 \pm 75$   |
| Misidentified jet $\rightarrow \tau$ | $510 \pm 23 \pm 86$           | $660 \pm 26 \pm 110$  |
| Misidentified $e \rightarrow \tau$   | $33 \pm 4 \pm 5$              | $34 \pm 4 \pm 6$      |
| Misidentified leptons                | $39 \pm 10 \pm 20$            | $90 \pm 10 \pm 34$    |
| All SM backgrounds                   | $1010 \pm 30 \pm 110$         | $1360 \pm 30 \pm 140$ |
| Data                                 | 880                           | 1219                  |
| $t \rightarrow bH^+$ (130 GeV)       | $220 \pm 6 \pm 29$            | $310 \pm 7 \pm 39$    |
| Signal+background                    | $1160 \pm 30 \pm 100$         | $1570 \pm 30 \pm 130$ |

**Table 3:** Expected event yields after all selection cuts in the  $\tau$ +lepton channel and comparison with  $4.6 \text{ fb}^{-1}$  of data. The numbers in the last two rows, for a hypothetical  $H^\pm$  signal with  $m_{H^\pm} = 130$  GeV, are obtained with  $\mathcal{B}(t \rightarrow bH^+) = 5\%$ . All other rows assume  $\mathcal{B}(t \rightarrow bW) = 100\%$ . Both statistical and systematic uncertainties are shown, in that respective order. [3]

## 5. Results, Limits and Combination

In absence of a significant excess above SM background estimations limits on  $\mathcal{B}(H^+ \rightarrow \tau^+ \nu) \times \mathcal{B}(H^+ \rightarrow \tau^+ \nu)$  are derived. Here the result of the lepton+jets analysis [7] is combined with the discussed,  $\tau$ +jets and  $\tau$ +lepton, analyses. It relies on the detection of lepton+jets decays of  $t\bar{t}$  events, where the charged lepton  $\ell$  (electron or muon) arises from leptonically decaying  $\tau$  from  $H^+ \rightarrow \tau_{\text{lep}}^+ \nu$ , while the jets arise from a hadronically decaying  $W$  boson, i.e.  $t\bar{t} \rightarrow b\bar{b}WH^+ \rightarrow b\bar{b}(q\bar{q}')(\tau_{\text{lep}}^+ \nu)$ , described in [3]. In order to test the compatibility of the data with background-only and signal+background hypotheses, a profile likelihood ratio, as described in [8], is used with the transverse Higgs mass,  $m_T^H$ , described in [9], (lepton+jets),  $E_T^{\text{miss}}(\tau$ +lepton) and  $m_T(\tau$ +jets) as the discriminating variables. The statistical analysis is based on a binned likelihood function for these distributions. No significant deviation from the SM prediction is observed in any of the

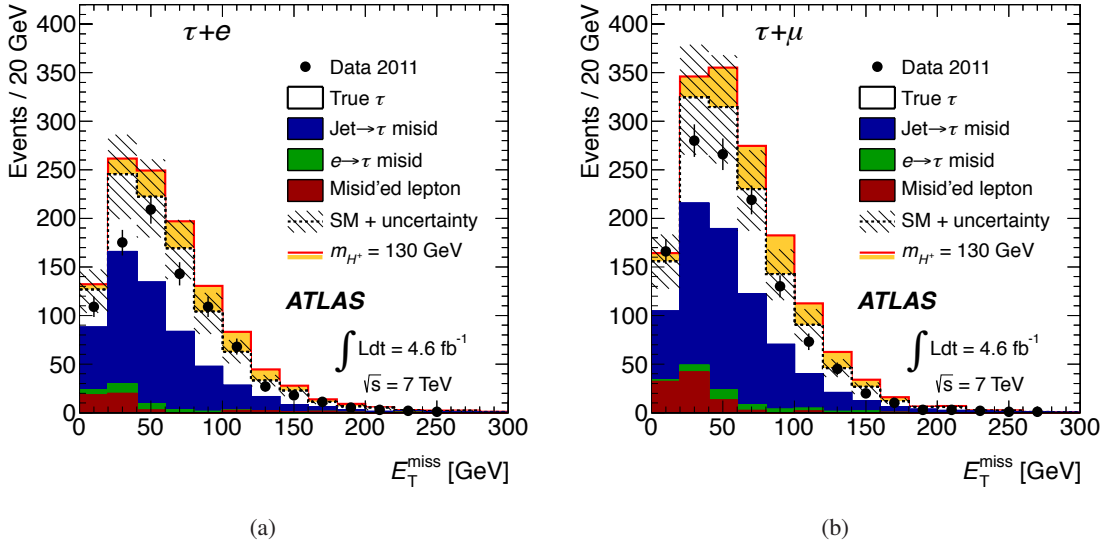


**Figure 5:**  $E_T^{\text{miss}}$  distributions after all selection cuts in the  $\tau$ +lepton channel, for (a)  $\tau$ +electron and (b)  $\tau$ +muon final states. The dashed lines correspond to the SM-only hypotheses and the hatched area around it shows the total uncertainty for the SM backgrounds. The solid line illustrates the predicted contribution of signal+background in the presence of a 130 GeV charged Higgs boson with  $\mathcal{B}(t \rightarrow bH^+) = 5\%$  and  $\mathcal{B}(H^\pm \rightarrow \tau^\pm \nu) = 100\%$ . The contributions of  $t\bar{t} \rightarrow b\bar{b}W^+W^-$  events in the backgrounds with true or misidentified  $\tau$  leptons are scaled down accordingly. [3]

investigated final states in  $4.6 \text{ fb}^{-1}$  of data. Exclusion limits are set on the branching fraction  $\mathcal{B}(t \rightarrow bH^+)$  and, in the context of the  $m_h^{\text{max}}$  scenario of the MSSM, on  $\tan\beta$ , by rejecting the signal hypothesis at the 95% confidence level (CL) using the  $\text{CL}_s$  procedure [10]. The 95% CL exclusion limits for the individual channels, as well as the combined limit, are shown in Figure 6 in terms of  $\mathcal{B}(t \rightarrow bH^+)$  under the assumption of  $\mathcal{B}(H^+ \rightarrow \tau^+ \nu) = 100\%$ . In Figure 7, the combined limit on  $\mathcal{B}(t \rightarrow bH^+) \times \mathcal{B}(H^+ \rightarrow \tau^+ \nu)$  is interpreted in the context of the  $m_h^{\text{max}}$  scenario of the MSSM.

## 6. Conclusions

Charged Higgs bosons have been searched for in  $t\bar{t}$  events, in the decay mode  $t \rightarrow bH^+$  followed by  $H^+ \rightarrow \tau^+ \nu$ . For this purpose, a total of  $4.6 \text{ fb}^{-1}$  of  $pp$  collision data at  $\sqrt{s} = 7 \text{ TeV}$  recorded in 2011 with the ATLAS experiment was used. Three final states were considered, two of these analyses were described in detail. The observed data are found to be in agreement with the SM predictions. Combining all three results and assuming  $\mathcal{B}(H^+ \rightarrow \tau^+ \nu) = 100\%$ , upper limits at the 95% confidence level have been set on the branching ratio  $\mathcal{B}(t \rightarrow bH^+)$  between 5% ( $m_{H^\pm} = 90 \text{ GeV}$ ) and 1% ( $m_{H^\pm} = 160 \text{ GeV}$ ). Interpreted in the context of the  $m_h^{\text{max}}$  scenario of the MSSM,  $\tan\beta$  above 12–26, as well as between 1 and 2–6, can be excluded in the mass range of  $90 \text{ GeV} < m_{H^\pm} < 150 \text{ GeV}$ . Search results will be updated utilizing the data taken in 2012 at  $\sqrt{s} = 8 \text{ TeV}$  at the LHC. It will be possible to improve the current results and also extend the  $m_{H^\pm}$  search range above the top-quark mass, entering the mass regime of heavy charged Higgs bosons.



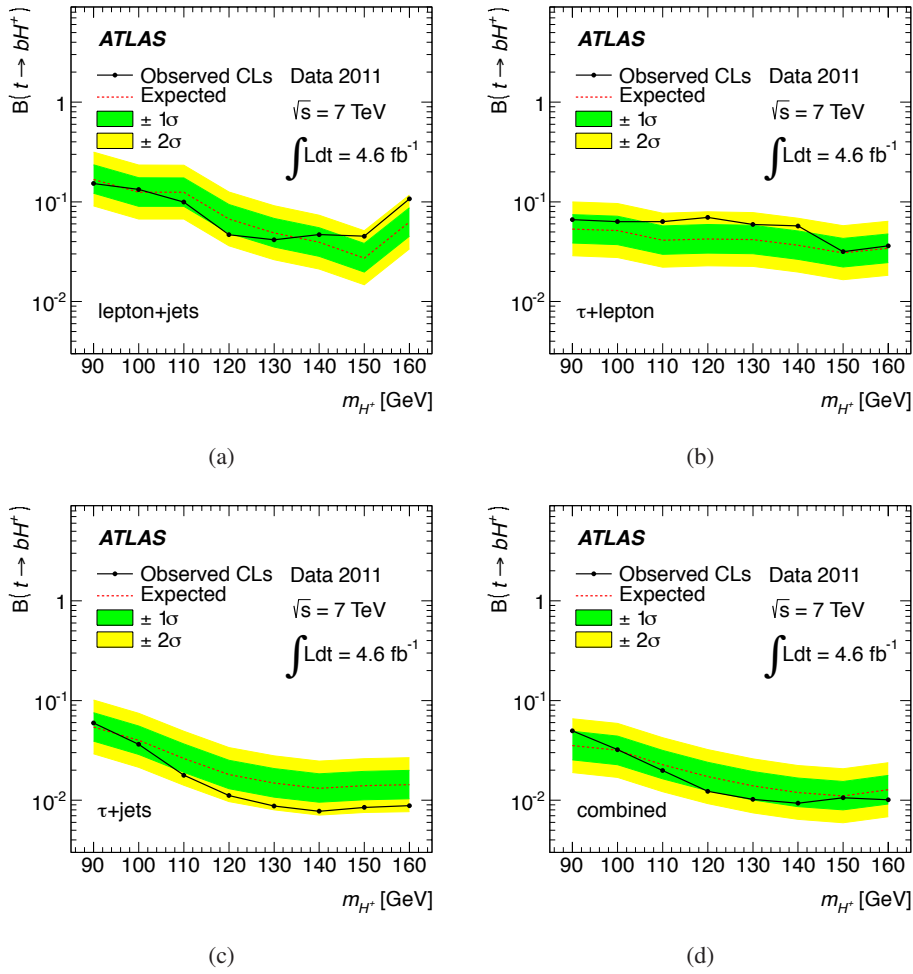


**Figure 6:** Expected and observed 95% CL exclusion limits on  $\mathcal{B}(t \rightarrow bH^+)$  for charged Higgs boson production from top quark decays as a function of  $m_{H^\pm}$ , assuming  $\mathcal{B}(H^+ \rightarrow \tau^+ \nu) = 100\%$ . Shown are the results for: (a) lepton+jets channel; (b)  $\tau$ +lepton channel; (c)  $\tau$ +jets channel; (d) their combination. [3]

## Acknowledgments

This work was supported by the German BMBF within the research network FSP-101 "Physics on the TeV Scale with ATLAS at the LHC", by the German Helmholtz Alliance "Physics At The Terascale" and the DFG research training group "Mass, Spectrum, Symmetry" (GK 1504).

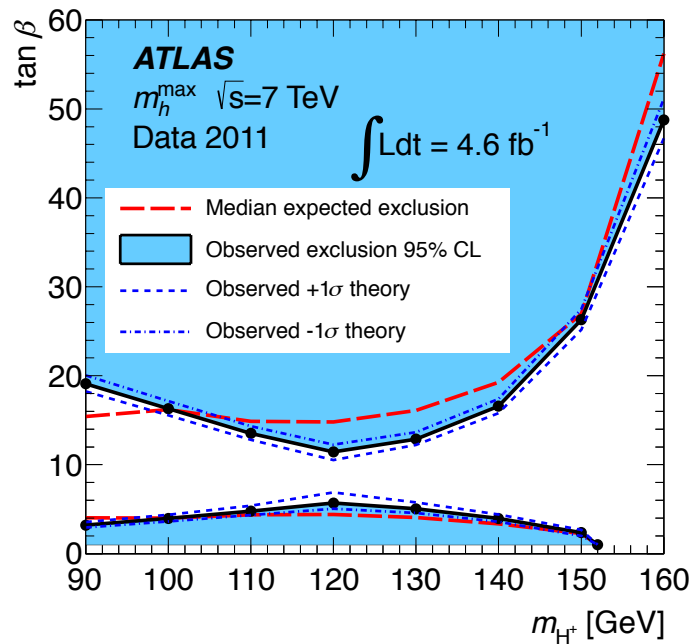


**Figure 7:** Combined 95% CL exclusion limits on  $\tan\beta$  as a function of  $m_{H^\pm}$ . Results are shown in the context of the MSSM scenario  $m_h^{\text{max}}$  for the region  $1 < \tan\beta < 60$  in which reliable theoretical predictions exist. The theoretical uncertainties as described in [3] are shown as well.

## References

- [1] Lee, T.D. "A Theory of Spontaneous T Violation" *Phys. Rev.* **D 8** (1973) 1226–1239.
- [2] ATLAS Collaboration "The ATLAS Experiment at the CERN Large Hadron Collider" *JINST* **3** (2008) S08003.
- [3] ATLAS Collaboration "Search for charged Higgs bosons decaying via  $H^\pm \rightarrow \tau^\pm + \nu$  in top quark pair events using  $pp$  collision data at  $\sqrt{s} = 7$  TeV with the ATLAS detector" *JHEP* **06** (2012) 039 [arXiv:1204.2760].
- [4] ATLAS Collaboration "Measurement of the Mis-identification Probability of  $\tau$  Leptons from Hadronic Jets and from Electrons" *ATLAS-CONF-2011-113*.
- [5] ATLAS Collaboration "Performance of the Reconstruction and Identification of Hadronic Tau Decays with ATLAS" *ATLAS-CONF-2011-152*.
- [6] ATLAS Collaboration "Performance of the ATLAS Trigger System in 2010" *Eur. Phys. J. C* **72** (2012) 1849 [arXiv:1110.1530].
- [7] Bernius, C. "Search for  $H^\pm$  and  $H^{\pm\pm}$  to other states than  $\tau_{\text{had}}\nu$  in ATLAS" *PoS (CHARGED2012) 009*, these proceedings.
- [8] Cowan, G., Cranmer, K., Gross, E. and Vitells, O. "Asymptotic formulae for likelihood-based tests of new physics" *Eur. Phys. J. C* **71** (2011) 1554 [arXiv:1007.1727].
- [9] Gross, E. and Vitells, O. "Transverse mass observables for charged Higgs boson searches at hadron colliders" *Phys. Rev.* **D 81** (2010) 055010 [arXiv:0907.5367].
- [10] Read, A. L. "Presentation of search results: The  $CL_s$  technique" *J. Phys.* **G 28** (2002) 2693.